How does the Nazca Ridge subduction influence the modern Amazonian foreland basin?

N. Espurt*]
P. Baby*] LMTG, Université de Toulouse, CNRS, IRD, OMP, 14 Avenue Edouard Belin, F-31400 Toulouse, France, and IRD, Convenio IRD-PERUPETRO, Calle Teruel 357, Miraflores, Lima 18, Peru
S. Brusset*]
M. Roddaz*] LMTG, Université de Toulouse, CNRS, IRD, OMP, 14 Avenue Edouard Belin, F-31400 Toulouse, France
W. Hermoza* PERUPETRO, Convenio IRD-PERUPETRO, Avenida Luis Aldana 320, San Boja, Lima 41, Peru
V. Regard*]
P.-O. Antoine*] LMTG, Université de Toulouse, CNRS, IRD, OMP, 14 Avenue Edouard Belin, F-31400 Toulouse, France
R. Salas-Gismondi* Museo de Historia Natural—UNMSM, Departamento de Paleontología de Vertebrados, Avenida Arenales 1256, Lima 14, Peru
R. Bolaños* PERUPETRO, Convenio IRD-PERUPETRO, Avenida Luis Aldana 320, San Boja, Lima 41, Peru

ABSTRACT

The subduction of an aseismic ridge has important consequences on the dynamics of the overriding upper plate. In the central Andes, the Nazca Ridge subduction imprint can be tracked on the eastern side of the Andes. The Fitzcarrald arch is the long-wavelength topography response of the Nazca Ridge flat subduction, 750 km inboard of the trench. This uplift is responsible for the atypical three-dimensional shape of the Amazonian foreland basin. The Fitzcarrald arch uplift is no older than Pliocene as constrained by the study of Neogene sediments and geomorphic markers, according to the kinematics of the Nazca Ridge subduction.

Keywords: Nazca Ridge, Amazonian foreland basin, Neogene, flat subduction, Fitzcarrald arch.

INTRODUCTION

Foreland basin evolution is related to fold-and-thrust belt propagation. The Amazon basin—the world's largest modern fluvial basin (Räsänen et al., 1992)—is currently an atypical foreland basin because the Amazonian foreland basin's three-dimensional configuration does not follow the foreland basin system model of DeCelles and Giles (1996). The Amazonian foreland basin is divided by the NE-SW–trending structural/morphologic Fitzcarrald arch (Räsänen et al., 1987) in two parts: the northern Amazonian foreland basin (Roddaz et al., 2005b) and the southern Amazonian foreland basin (Roddaz et al., 2005b; Baby et al., 1999), both driven by Andean thrust loading. The Fitzcarrald arch corresponds to a widespread dissected relief. The Nazca Ridge is N45°E trending and oblique to the N78°E present-day plate convergence. It is one of the major oceanic ridges subducting below the South American plate, with a bathymetric relief of on average 1500 m above the adjacent seafloor of the Nazca plate, and has a maximum width of 200 km (Woods and Okal, 1994). Ridge subduction signatures have only been tracked in the Pacific forearc area (von Huene and Suess, 1988; Hsu, 1992; Macharé and Ortlieb, 1992; von Huene et al., 1996; Gutscher et al., 1999a; Le Roux et al., 2000; Hampel, 2002), but never for the eastern Amazonian side of the Andes. The aim of this paper is to show relationships between the Nazca Ridge subduction and the Fitzcarrald arch in the Amazonian foreland basin from the analysis of geomorphic markers and lithospheric data.

*E-mails: espurt@lmtg.obs-mip.fr; pbaby@ird.fr; brusset@lmtg.obs-mip.fr; mroddaz@lmtg.obs-mip.fr; whermoza@perupetro.com.pe; regard@lmtg.obs-mip.fr; poa@lmtg.obs-mip.fr; rodsalasgis@yahoo.com; rbolanos@perupetro.com.pe.

MORPHOLOGY OF THE FITZCARRALD ARCH

The structural/morphologic Fitzcarrald arch extends from southern Peru to western Brazil and constitutes a major geomorphic feature spreading more than 4×10^5 km^2 in Amazonia, occurring at ~750 km from the trench (Fig. 1). It extends east of the Subandean thrust front where no thrust deformation occurs (Figs. 1 and 2). The Fitzcarrald arch separates the foredeeps of the northern Amazonian foreland basin and southern Amazonian foreland basin (Roddaz et al., 2005b; Baby et al., 1999) and to the east is bounded by the subsiding eastern Amazon basin (Kronberg et al., 1998). The northern Amazonian foreland basin and southern Amazonian foreland basin are ~120 masl and ~150 masl, respectively, and the Fitzcarrald arch has a mean uplifted surface ~600 masl. The digital elevation model (Fig. 2A) shows that the Fitzcarrald arch disturbs the present-day drainage network of the Amazon basin, generating a radial drainage. The arch defines three drainage basins: rivers of the northern Amazonian foreland basin to the north, rivers of the eastern Amazon basin to the east, and rivers of the southern Amazonian foreland basin to the south. The Fitzcarrald arch is incised by these rivers, and the oldest outcropping sediments are Neogene in age. Recent studies of both sides of the arch (Fig. 2A) show Late Miocene tidal deposits (Räsänen et al., 1995; Hovikoski et al., 2005; Gingras et al., 2002; Rebata et al., 2006). These tidal deposits show that this part of the Amazonian foreland basin was a subsiding foredeep during the Late Miocene. They are currently overlain by Pliocene and Quaternary fluvial deposits. The digital elevation model (Fig. 2A) enables us to observe beddings of such deposits where they are parallel to the topographic surfaces. The NW-SE–trending profile of the arch (Fig. 2B) demonstrates that beddings organize asymmetrically. On the northwestern flank of the arch, beddings dip 0.3° northwestward. In contrast, the southeastern flank of the arch presents several less-tilted beddings dipping 0.1° to the southeast (Figs. 2A and 2B).

LITHOSPHERIC STRUCTURES

Numerous two-dimensional seismic lines and wells have been acquired by oil companies on the Fitzcarrald arch because it includes the massive Camisea gas field (Fig. 2A). To illustrate the uplift of the Fitzcarrald arch, we used four seismic reflection profiles (HIS-20, 85-UB-106, TOT-220, and 96-MGLP-106) provided by Perupetro S.A. to construct a synthetic 340 km long section perpendicular to the axis of the arch (Fig. 3). Reflectors have been calibrated using the Mashansha and Panguana wells (see Fig. 2A for location), which reach the pre-Mesozoic basement. This composite seismic section shows a bulge at a lithospheric-scale wavelength (340 km minimum). This bulge is underlain by 2.5-km-thick Cretaceous and Cenozoic strata of nearly constant thickness. Seismic data show Paleozoic structures (Manu arch) unconformably overlain by Cretaceous strata. The Neogene is partially eroded and exposed in both flanks of the Fitzcarrald arch. No thickness variation in the Neogene sediments, which could support a synsedimentary Neogene uplift of the Fitzcarrald arch, is visible.

Figure 1. Geodynamic setting of the Peruvian Andes and its associated Amazonian foreland basin. The base map is produced using bathymetric data from the Geosat and ERS-1 spacecraft (Smith and Sandwell, 1997) and elevation data from NASA (National Aeronautics and Space Administration) SRTM (Shuttle Radar Topographic Mission) Gtopo 30. Note that the western part of the Amazon basin consists of two main subsiding basins—the northern Amazonian foreland basin (NAFB) and the southern Amazonian foreland basin (SAFB)—separated by the Fitzcarrald arch. To the east, the Fitzcarrald arch is bounded by the eastern Amazon basin (EAB). This arch is superimposed on the present-day reconstruction of the subducted part of the Nazca Ridge (Hampel, 2002, modified). The ridge reconstruction at 11.2 Ma is shown (Hampel, 2002). The easternmost edge of the Nazca Ridge represented by dotted line is not involved in the flat slab segment. The black dashed line (E–F) locates the deep seismicity section of Figure 5. Depth contours to Wadati-Benioff zone are from Gutscher et al. (1999b), and plate convergence vector is from Gripp and Gordon (2002).

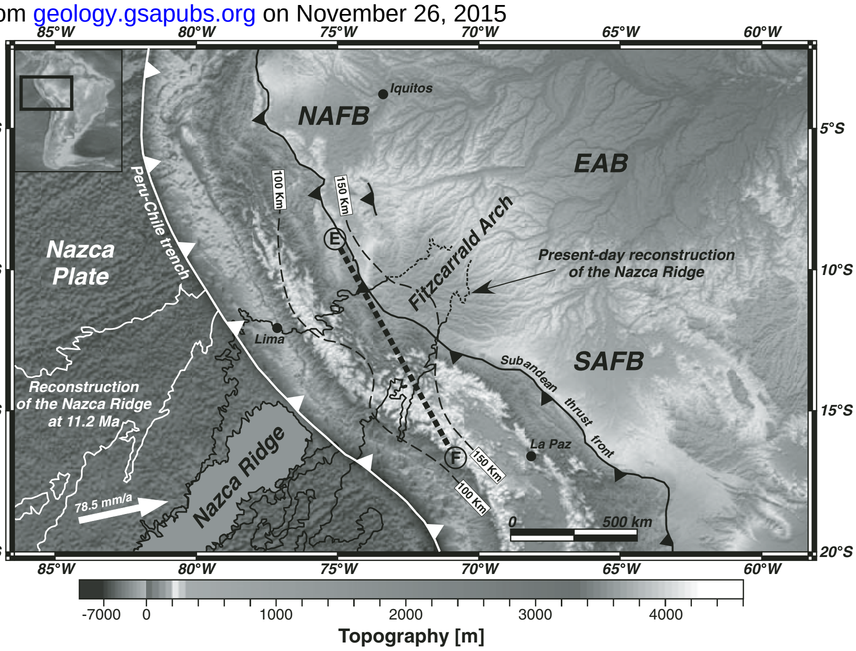

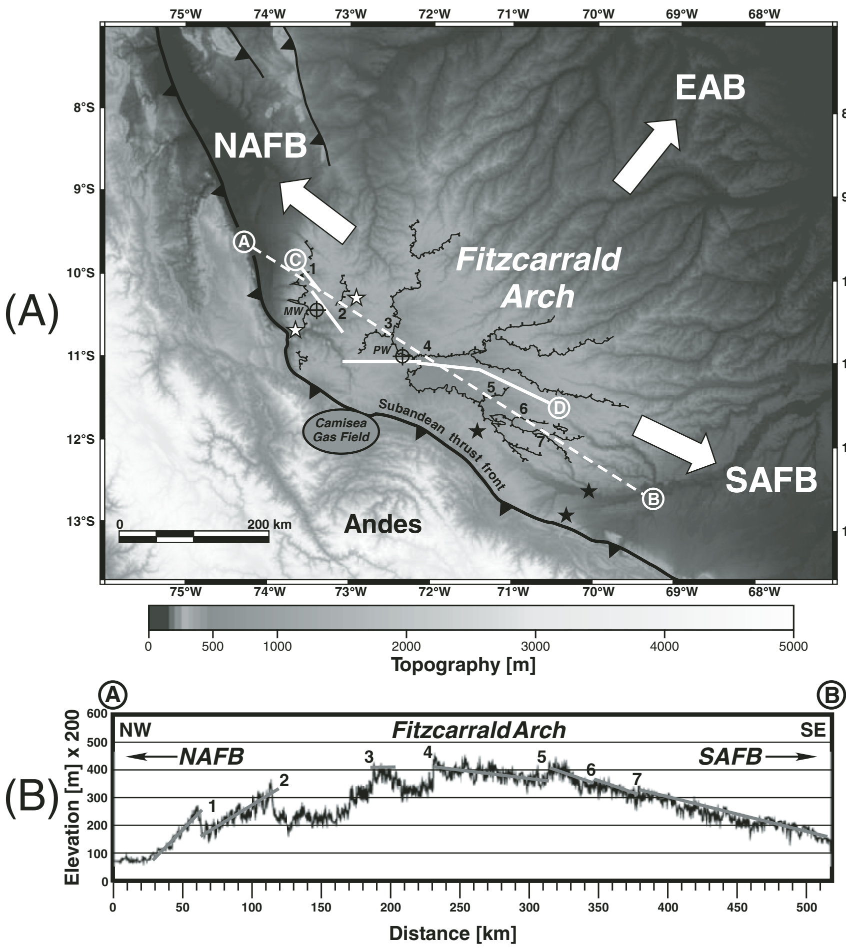

Figure 2. A: Digital elevation model of the Fitzcarrald arch (DEM SRTM 90 m from NASA data). The arch is characterized by a radial drainage network (white arrows) that defines the northern Amazonian foreland basin (NAFB), southern Amazonian foreland basin (SAFB), and eastern Amazon basin (EAB). White lines show the location of the seismic lines used to build the composite seismic section (C–D) of Figure 3. Cross-points MW and PW locate the Mashansha and Panguana wells, respectively. Bedding boundaries are indicated by black lines with bars toward the scarp. Stars indicate study zones of Neogene outcrops: black stars from Hovikoski et al. (2005), white stars from our study. B: Topographic profile (dashed white line A–B) perpendicular to the axis of the arch showing the asymmetric shape of the arch. The asymmetric shape of the arch is demonstrated by bedding dip where parallel to the topography (gray lines). The scarps are numbered from 1 to 7.

The three-dimensional Wadati-Benioff zone of the Nazca slab (Fig. 4), built by hypocenter relocation database from Engdahl et al. (1998), shows that the Nazca Ridge buoyancy (Vogt et al., 1976; Kelleher and McCann, 1976) controls the dynamics and the geometry of the Nazca slab beneath the South American lithosphere (Gutscher et al., 1999b). The subducting lithosphere descends at an angle of ~30° from the trench to a depth of 100–120 km, then extends horizontally beneath the South American lithosphere to sink in the upper mantle 700 km farther from the trench. The reconstruction of the Nazca Ridge beneath the South American lithosphere (Fig. 1) (Hampel, 2002) indicates that the Nazca Ridge supports an ~785-km-long flat segment reaching the Amazonian foreland basin beneath the Fitzcarrald arch. The lithospheric section of the Nazca flat slab segment beneath the Andes (Fig. 5B) (Gutscher et al., 1999b), shows an intermediate-depth seismic gap that is interpreted as the subducted continuation of the Nazca Ridge (Gutscher et al., 1999b; Hampel, 2002). The curvature of the Nazca slab linked to the buoyant Nazca Ridge segment is of the same order of magnitude as, and superimposed on, that of the Fitzcarrald arch bulge (Fig. 5A).

TIMING OF THE FITZCARRALD ARCH UPLIFT

In the Peruvian forearc, the Nazca Ridge subduction started at 11.2 Ma (Fig. 1) (Hampel, 2002). Its southward migration between 11°S and 17°S has been recorded in the geomorphology and sedimentary facies of the forearc and accompanied by an uplift of more than 500 m of the Pacific coast (von Huene and Suess, 1988; Hsu, 1992; Macharé and Ortlieb, 1992; Le Roux et al., 2000; Hampel, 2002). In the Amazonian foreland basin, recent studies (Räsänen et al.,

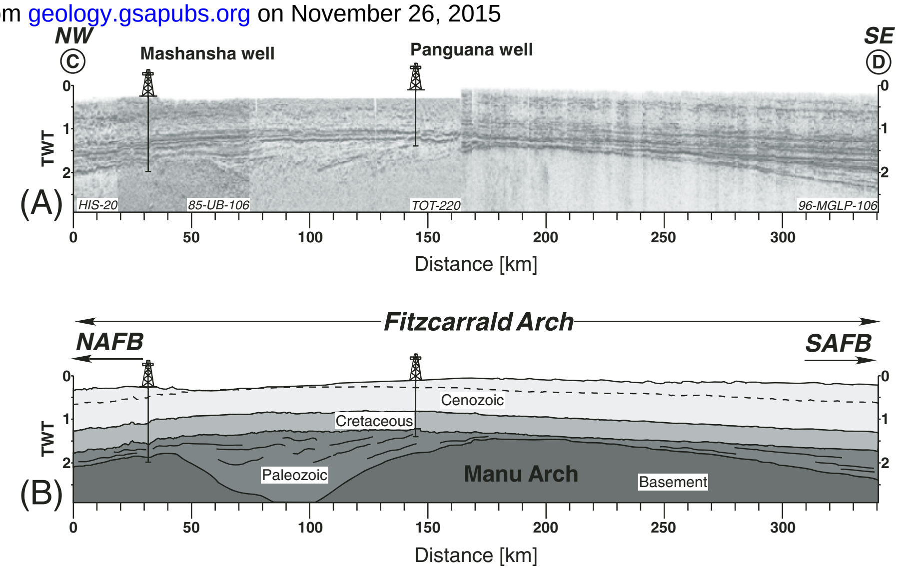

Figure 3. A: Composite seismic reflection profile (courtesy of Perupetro S.A.) crossing the Fitzcarrald arch (C–D; see location in Fig. 2A). B: The Fitzcarrald arch is underlain by a constant thickness of Cretaceous and Cenozoic deposits. A dashed black reflector shows the base of Neogene strata. The locations of the projected Mashansha and Panguana wells are shown. The seismic regional profile shows Paleozoic sedimentary basins and pre-Cretaceous structures (Manu arch). These structures present a wavelength of ~100 km. Seismic profile demonstrates that these older structures have been eroded and sealed by Cretaceous strata, and subsequently uplifted and involved in the larger structure of the Fitzcarrald arch. NAFB—northern Amazonian foreland basin; SAFB—southern Amazonian foreland basin; TWT—two-way time.

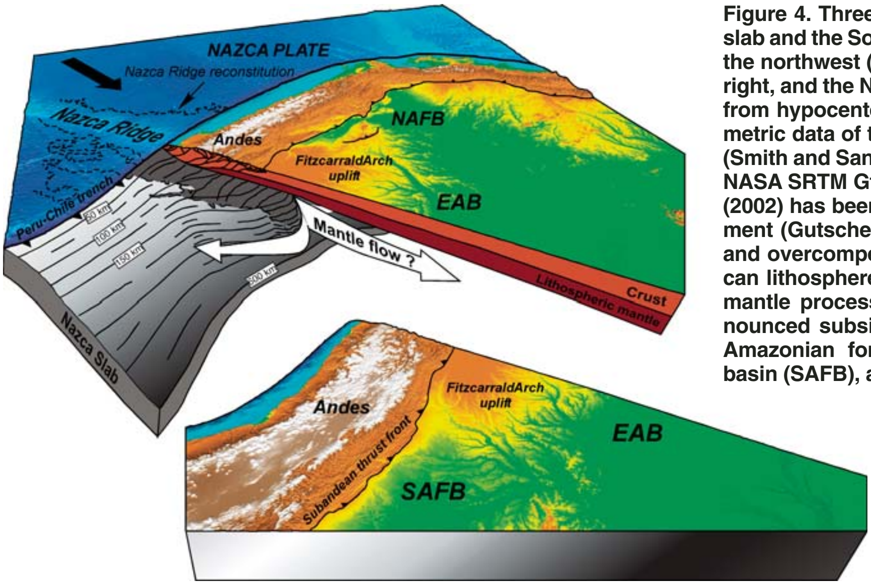

Figure 4. Three-dimensional lithospheric-scale diagram of the Nazca slab and the South American plate. The perspective view looks toward the northwest (with the Andes in the middle, the Amazon basin to the right, and the Nazca plate to the left). The Nazca slab geometry is built from hypocenter relocation database of Engdahl et al. (1998). Bathymetric data of the Nazca plate from the Geosat and ERS-1 spacecraft (Smith and Sandwell, 1997), and elevation data of South America from NASA SRTM Gtopo 30. The Nazca Ridge reconstruction from Hampel (2002) has been draped onto the Nazca slab. The Nazca flat slab segment (Gutscher et al., 1999b) reaches the Amazonian foreland basin and overcompensates the thrust loading flexure of the South American lithosphere. It induces an eastward shift of the dynamic loading mantle processes coupled to the subducting slab, generating pronounced subsidence in basins all around the arch, in the northern Amazonian foreland basin (NAFB), southern Amazonian foreland basin (SAFB), and eastern Amazon basin (EAB).

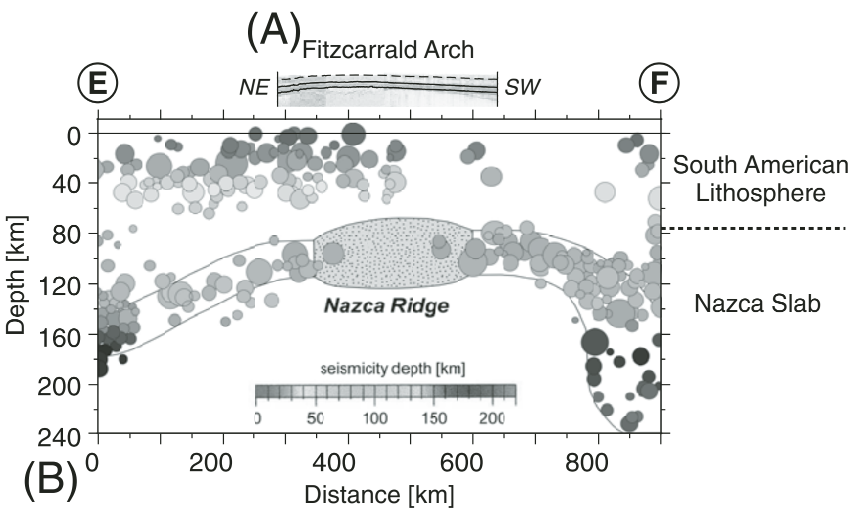

Figure 5. Deep seismicity trench-parallel section (Gutscher et al., 1999b, modified) (990 km long and 240 km deep; see Fig. 1 for location) showing the geometry of the Nazca slab beneath the South American lithosphere (B). We note that the Fitzcarrald arch bulge (A) correlates well the interpreted position of the buoyant subducted Nazca Ridge (B). Circle diameter refers to the earthquake magnitudes.

1995; Gingras et al., 2002; Hermoza et al., 2005; Hovikoski et al., 2005; Roddaz et al., 2005a; Rebata et al., 2006) show that during the Late Miocene, the Amazonian foreland basin constituted a four-component foreland basin system sensu DeCelles and Giles (1996). Sedimentologic data indicate that the Fitzcarrald arch uplift did not exist in the Late Miocene. The Fitzcarrald area was included in the subsiding foredeep depozone and subject to marine incursions. The occurrence of the flat slab segment, linked to the Nazca Ridge subduction (Gutscher et al., 2000), has been correlated with the cessation of arc volcanism activity (Nur and Ben-Avraham, 1981; McGeary et al., 1985; Gutscher et al., 2000). In the Peruvian Andes adjacent to the Amazonian foreland basin, arc volcanism ceased 4 m.y. ago (Soler and Bonhomme, 1990; Rosenbaum et al., 2005). The flattening process propagates from the trench eastward to the previously subducted segment of the oceanic lithosphere. As the cessation of arc volcanism occurred 4 m.y. ago in response to flat slab subduction, it is unlikely that the Fitzcarrald arch uplift is older than 4 Ma.

Geomorphic and lithospheric data show that the uplift of the long-wavelength Fitzcarrald arch is due to the subduction of the buoyant Nazca Ridge. As a result, the flexure of the South American lithosphere is overcompensated (Fig. 4), and a four-component foreland basin system has been unable to form since 4 Ma. The recent deformation of the Fitzcarrald arch is characterized by vertical motions as recorded by the radial modern drainage network and the opposite dips of recent fluvial deposits on both sides of the arch.

CONCLUSIONS

The Fitzcarrald arch uplift occurred since 4 Ma in response to the Nazca Ridge flat subduction. The Nazca Ridge flat subduction is responsible for the atypical three-dimensional geometry of the Amazonian foreland basin and separated the northern Amazonian foreland basin from the southern Amazonian foreland basin. Present-day rapid and large rates of subsidence are observed in the northern Amazonian foreland basin, southern Amazonian foreland basin, and eastern Amazon basin (Räsänen et al., 1987; Kronberg et al., 1998; Baby et al., 1999; Aalto et al., 2006). The Nazca Ridge flat subduction will disturb mantle flow beneath the Amazon basin (Fig. 4), thus creating additional dynamic loading (Mitrovica et al., 1989; Pysklywec and Mitrovica, 2000). This control of the Amazonian foreland basin geometry by the flat subduction of the Nazca Ridge might be one of the decisive factors that triggered modification of large-scale sedimentological and hydrological processes in the Amazon basin during the last 4 m.y.

ACKNOWLEDGMENTS

This research project is led thanks to the Institut de Recherche pour le Développement–Perupetro S.A. research agreement, and supported by IRD (UR 154) and French Institut National des Sciences de l'Univers-Centre National de la Recherche Scientifique programs DyETI (Dynamique et Evolution de la Terre Interne) and ECLIPSE II (Environnement et CLImat du Passé: hiStoire et Evolution). We thank J. Martinod, J.C. Soula, and P. Soler for helpful discussions. We also thank M.-A. Gutscher and an anonymous reviewer for constructive and critical comments.

REFERENCES CITED

Aalto, R., Dunne, T., and Guyot, J.L., 2006, Geomorphic controls on Andean denudation rates: Journal of Geology, v. 114, p. 85–99, doi: 10.1086/498101.

Baby, P., Guyot, J.L., Deniaud, Y., Zubieta, D., Christophoul, F., and Rivadeneira, M., 1999, The High Amazonian Basin: Tectonic control and mass balance, *in* HiBAm (Hydrology and geochemistry of the Amazon BAsin), eds., Hydrological and Geochemical Process in Large-Scale River Basins: Manaus (Brazil), International Symposium MANAUS 99, November 15-19, Extended Abstracts, CD-ROM.

DeCelles, P.G., and Giles, K.A., 1996, Foreland basin systems: Basin Research, v. 8, p. 105–123, doi: 10.1046/j.1365-2117.1996.01491.x.

Engdahl, E.R., van der Hilst, R.D., and Buland, R., 1998, Global teleseismic earthquake relocation with improved travel times and procedures for depth relocation: Bulletin of the Seismological Society of America, v. 88, p. 722–743.

Gingras, M.K., Räsänen, M.E., Pemberton, S.G., and Romero, L.P., 2002, Ichnology and sedimentology reveal depositional characteristics of bay margin parasequences in the Miocene Amazonian foreland basin: Journal of Sedimentary Research, v. 72, p. 871–883.

Gripp, A.E., and Gordon, R.G., 2002, Young tracks of hotspots and current plate velocities: Geophysical Journal International, v. 150, p. 321–361, doi: 10.1046/j.1365-246X.2002.01627.x.

Gutscher, M.-A., Malavielle, J., Lallemand, S., and Collot, J.-Y., 1999a, Tectonic segmentation of the North Andean margin: Impact of the Carnegie Ridge collision: Earth and Planetary Science Letters, v. 168, p. 255–270, doi: 10.1016/S0012-821X(99)00060-6.

Gutscher, M.-A.., Olivet, J.L., Aslanian, D., Eissen, J.P., and Maury, R., 1999b, The "lost Inca Plateau": Cause of flat subduction beneath Peru?: Earth and Planetary Science Letters, v. 171, p. 335–341, doi: 10.1016/S0012-821X(99)00153-3.

Gutscher, M.-A., Spakman, W., Bijwaard, H., and Engdalh, E.R., 2000, Geodynamics of flat subduction: Seismicity and tomographic constraints from the Andean margin: Tectonics, v. 19, p. 814–833, doi: 10.1029/1999TC001152.

Hampel, A., 2002, The migration history of the Nazca Ridge along the Peruvian active margin: A re-evaluation: Earth and Planetary Science Letters, v. 203, p. 665–679, doi: 10.1016/S0012-821X(02)00859-2.

Hermoza, W., Brusset, S., Baby, P., Gil, W., Roddaz, M., Guerrero, N., and Bolaños, R., 2005, The Huallaga foreland basin evolution: Thrust propagation in a deltaic environment, northern Peruvian Andes: Journal of South American Earth Sciences, v. 19, p. 21–34, doi: 10.1016/j.jsames.2004.06.005.

Hovikoski, J., Räsänen, M., Gingras, M., Roddaz, M., Brusset, S., Hermoza, W., Pittman, L.R., and Lertola, K., 2005, Miocene semi-diurnal tidal rhythmites in Madre de Dios, Peru: Geology, v. 33, p. 177–180, doi: 10.1130/G21102.1.

Hsu, J.T., 1992, Quaternary uplift of the Peruvian coast related to the subduction of the Nazca Ridge: 13.5 to 15.6 degrees south latitude: Quaternary International, v. 15/16, p. 87–97.

Kelleher, J., and McCann, W., 1976, Buoyant zones, great earthquakes, and unstable boundaries of subduction: Journal of Geophysical Research, v. 26, p. 4885–4897.

Kronberg, B.I., Fralick, P.W., and Benchimol, R.E., 1998, Late Quaternary sedimentation and palaeohydrology in the Acre foreland basin, SW Amazonia: Basin Research, v. 10, p. 311–323, doi: 10.1046/j.1365-2117.1998.00067.x.

Le Roux, J.P., Tavares Correa, C., and Alayza, F., 2000, Sedimentology of the Rimac-Chillon alluvial fan at Lima, Peru, as related to Plio-Pleistocene sea level changes, glacial cycles and tectonics: Journal of South American Earth Sciences, v. 13, p. 499–510, doi: 10.1016/S0895-9811(00)00044-4.

Macharé, J., and Ortlieb, L., 1992, Plio-Quaternary vertical motions and the subduction of the Nazca Ridge, central coast of Peru: Tectonophysics, v. 205, p. 97–108, doi: 10.1016/0040-1951(92)90420-B.

McGeary, S., Nur, A., and Ben-Avraham, Z., 1985, Spatial gaps in arc volcanism: The effect of collision or subduction of oceanic plateaus: Tectonophysics, v. 119, p. 195–221, doi: 10.1016/0040-1951(85)90039-3.

Mitrovica, J.X., Beaumont, C., and Jarvis, G.T., 1989, Tilting of continental interiors by the dynamical effects of subduction: Tectonics, v. 8, p. 1078–1094.

Nur, A., and Ben-Avraham, Z., 1981, Volcanic gaps and the consumption of aseismic ridges in South America, *in* Kulm, L.D., et al., eds., Nazca plate: Crustal formation and Andean convergence: Geological Society of America Memoir 154, p. 729–740.

Pysklywec, R.N., and Mitrovica, J.X., 2000, Mantle flow mechanisms of epeirogeny and their possible role in the evolution of the Western Canada Sedimentary Basin: Canadian Journal of Earth Sciences, v. 37, p. 1535–1548, doi: 10.1139/cjes-37-11-1535.

Räsänen, M.E., Salo, J.S., and Kalliola, R.J., 1987, Fluvial perturbance in the western Amazon basin: Regulation by long-term sub-Andean tectonics: Science, v. 238, p. 1398–1401.

Räsänen, M.E., Neller, R., Salo, J., and Jungner, H., 1992, Recent and ancient fluvial deposition systems in the Amazonian foreland basin, Peru: Geological Magazine, v. 129, p. 293–306.

Räsänen, M.E., Linna, A.M., Santos, J.C.R., and Negri, F.R., 1995, Late Miocene tidal deposits in the Amazonian foreland basin: Science, v. 269, p. 386–390, doi: 10.1126/science.269.5222.386.

Rebata, L.A., Räsänen, M.E., Gingras, M.K., Vieira, V., Jr., Barberi, M., and Irion, G., 2006, Sedimentology and ichnology of tide-influenced Late Miocene successions in western Amazonia: The gradational transition between the Pebas and Nauta Formations: Journal of South American Earth Sciences, v. 21, p. 96–119, doi: 10.1016/j.jsames.2005.07.011.

Roddaz, M., Baby, P., Brusset, S., Hermoza, W., and Darrozes, J., 2005a, Forebulge dynamics and environmental control in western Amazonia: The case study of the arch of Iquitos (Peru): Tectonophysics, v. 399, p. 87–108, doi: 10.1016/j.tecto.2004.12.017.

Roddaz, M., Viers, J., Brusset, S., Baby, P., Brusset, S., and Hérail, G., 2005b, Sediment provenances and drainage evolution of the Neogene Amazonian foreland basin: Earth and Planetary Science Letters, v. 239, p. 57–78.

Rosenbaum, G., Giles, D., Saxon, M., Betts, P.G., Weinberg, R.F., and Duboz, C., 2005, Subduction of the Nazca Ridge and the Inca Plateau: Insights into the formation of ore deposits in Peru: Earth and Planetary Science Letters, v. 239, p. 18–32, doi: 10.1016/j.epsl.2005.08.003.

Smith, H.F.W., and Sandwell, D.T., 1997, Global sea floor topography from satellite altimetry and ship depth soundings: Science, v. 277, p. 1956–1961, doi: 10.1126/science.277.5334.1956.

Soler, P., and Bonhomme, M.G., 1990, Relation of magmatic activity to plate dynamics in central Peru from Late Cretaceous to present: Geological Society of America Special Paper 241, p. 173–192.

Vogt, P.R., Lowrie, A., Bracey, D., and Hey, R., 1976, Subduction of aseismic oceanic ridges: Effects on shape, seismicity, and other characteristics of consuming plate boundaries: Geological Society of America Special Paper 172, p. 1–59.

von Huene, R., and Suess, E., 1988, Leg 112 shipboard scientific party, Ocean Drilling Program Leg 112, Peru continental margin: Part 1, tectonic history: Geology, v. 16, p. 934–938, doi: 10.1130/0091-7613(1988)016<0934:ODPLPC>2.3.CO;2.

von Huene, R., Pecher, I.A., and Gutscher, M.-A., 1996, Development of the accretionary prism along Peru and material flux after subduction of Nazca Ridge: Tectonics, v. 15, p. 19–33.

Woods, M.T., and Okal, E.A., 1994, The structure of the Nazca Ridge and Sala y Gomez seamount chain from dispersion of Rayleigh waves: Geophysical Journal International, v. 117, p. 205–222.

Manuscript received 26 July 2006
Revised manuscript received 26 January 2007
Manuscript accepted 7 February 2007

Printed in USA

Geology

How does the Nazca Ridge subduction influence the modern Amazonian foreland basin?

N. Espurt, P. Baby, S. Brusset, M. Roddaz, W. Hermoza, V. Regard, P.-O. Antoine, R. Salas-Gismondi and R. Bolaños

Geology 2007;35;515-518
doi: 10.1130/G23237A.1